DEUTSCHES ELEKTRONEN-SYNCHROTRON DESY

DESY SR-83-12
August 1983

EXPERIMENTAL PROGRESS IN ATOMIC AND MOLECULAR PHOTOIONIZATION

by

B.F. Sonntag

University of Hamburg

ISSN 0723-7979

NOTKESTRASSE 85 · 2 HAMBURG 52

To be sure that your preprints are promptly included in the HIGH ENERGY PHYSICS INDEX , send them to the following address (if possible by air mail) :

DESY
Bibliothek
Notkestrasse 85
2 Hamburg 52
Germany

ISSN 0723-7979

EXPERIMENTAL PROGRESS IN ATOMIC AND MOLECULAR PHOTOIONIZATION

B. F. Sonntag
University of Hamburg, Hamburg Germany

The progress in atomic and molecular ionization by single photon impact will be showcased by presenting recent experimental results.

INTRODUCTION

Photoionization studies form an excellent tool to probe the states and the dynamics of atoms and molecules (1-4). The steady improvements of the experimental techniques (5) have enabled us to unravel more and more details and thereby promoted our understanding of these many particle systems. In the following we will concentrate on the photon energy range 10 eV $\leq \hbar\omega \leq$ 10 keV. The scope of the discussion is outlined in Fig. 1. The four columns give the structure of the paper.

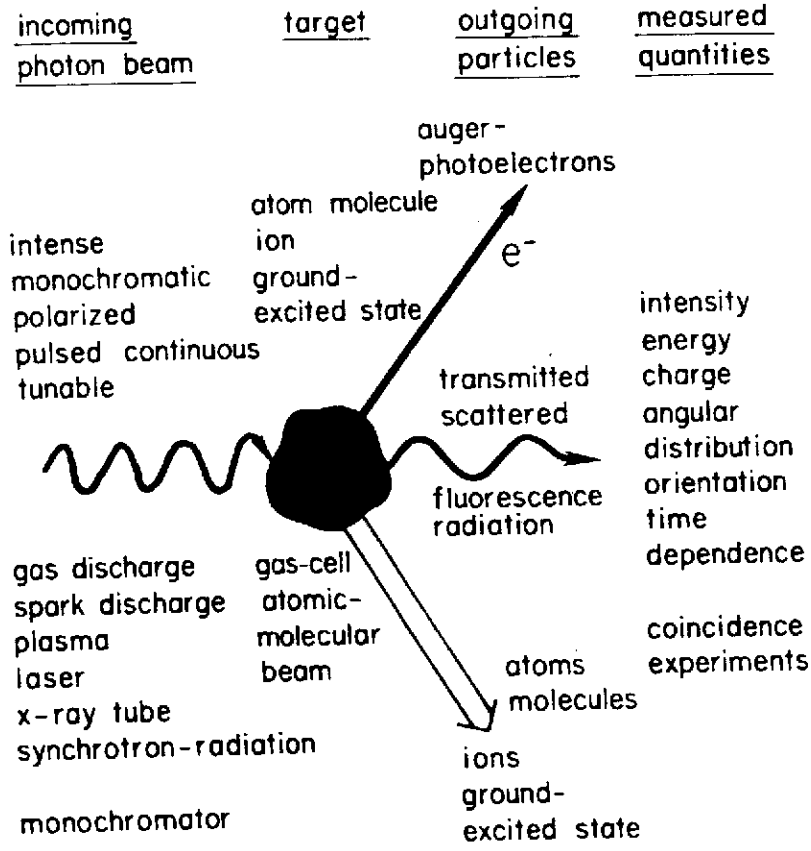

Figure 1
Scheme of photoionization studies

LIGHT SOURCE

Intense monochromatic polarized light beams are the perequisite of todays photoionization studies (1, 4, 5). For many experiments the combination of an electron storage ring and a monochromator has been proven the optimal source (5, 6). On the other hand there is a continuous improvement of conventional light sources, which in many cases renders them attractive alternatives. For a comparison of the various types of light sources the reader is referred to a recent article (7). Great progress has been made in the development of VUV sources based on frequency mixing of powerful laser radiation (8). These sources are capable of delivering a very high photon flux within a very narrow energy band. The radiation is well collimated, polarized, coherent and tunable within a limited energy range. The impact the advent of wiggler and undulator sources (9) will have on photoionization experiments can be judged from the experiments performed up to now. The envisaged development of these sources will make experiments feasable, which are out of reach today. To illustrate the perspectives we will briefly discuss the threshold studies of multivacancy processes in the Kβ region of Ar (10). The experiment used synchrotron radiation produced in the six pole wiggler at the Stanford Synchrotron Radiation Laboratory. The incident radiation was monochromatized by a focusing two-crystal monochromator (11). The fluorescent radiation was analyzed in a focusing spectrometer with a linear position sensitive detector. In Fig. 2 a schematic diagram of Argon single-(left) and double-(right) vacancy transitions expected to produce X-ray emission near Kβ energy is presented.

Figure 2
Schematic diagram of the principal transitions in the Kβ energy region

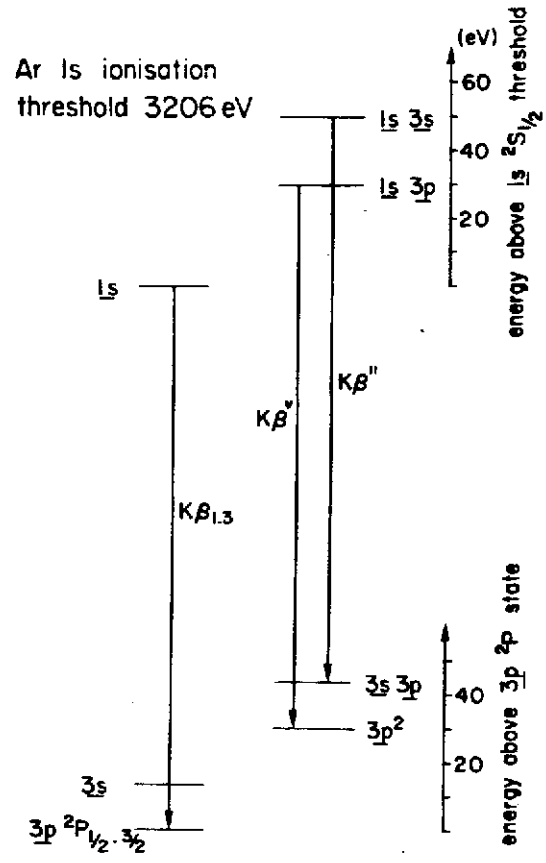

Multiple electron excitations give rise to the structure detected in the photoabsorption spectrum in the region 10 to 50 eV above the Ar 1s ionization threshold. This spectrum is shown in Fig. 3. The energy positions obtained by Hartree-Fock calculations (above) and by the Z+1 approximation (below) are indicated (hole states are under lined). The structures

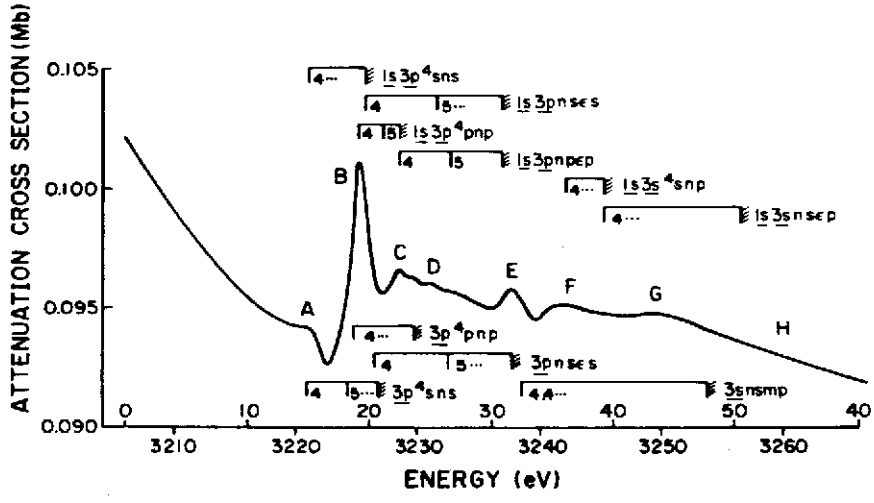

Figure 3
Absorption structure above the Ar K-edge (from Ref. 10)

A-D are ascribe to the simultaneous excitation of a 1s electron and a 3p electron. The onset of the simultaneous creation of a 1s and a 3s hole is located at the feature E. The study of the K-emission spectra excited by X-rays below and above the multiple excitation thresholds provides the opportunity to correlate the effects in emission and absorption spectra. This greatly enhances the possibility to disentangle the various processes resulting in satellite emission. A spectrum obtained at high excitation energies (Fig. 4a) shows three prominent features, traditionally labeled $K\beta_{1,3}$ (3190 eV) $K\beta'$ (3193.7 eV) and Kβ" (3197.9 eV). However at excitation energies between ~ 20 and ~60 eV above threshold the Kβ" feature disappears (Fig. 4b). Between threshold and +20 eV above both satellites are absent leaving only the $K\beta_{1,3}$ diagram line (Fig. 4c). The presence of $K\beta'$ only at excitation energies sufficient to create 1s3p hole states confirm this feature as a $1s3p \rightarrow 3p^2$ transition. The appearance of Kβ" at energies above the 1s3s threshold implies that it is due to $1s3s \rightarrow 3s3p$ transitions (see Figs. 2 and 3). Multi-electron effects connected with the 1s ionization threshold have been subject to several studies. Recently new results have been reported on double excitations in high resolution K-absorption spectra of Ne (12) and Na (13).

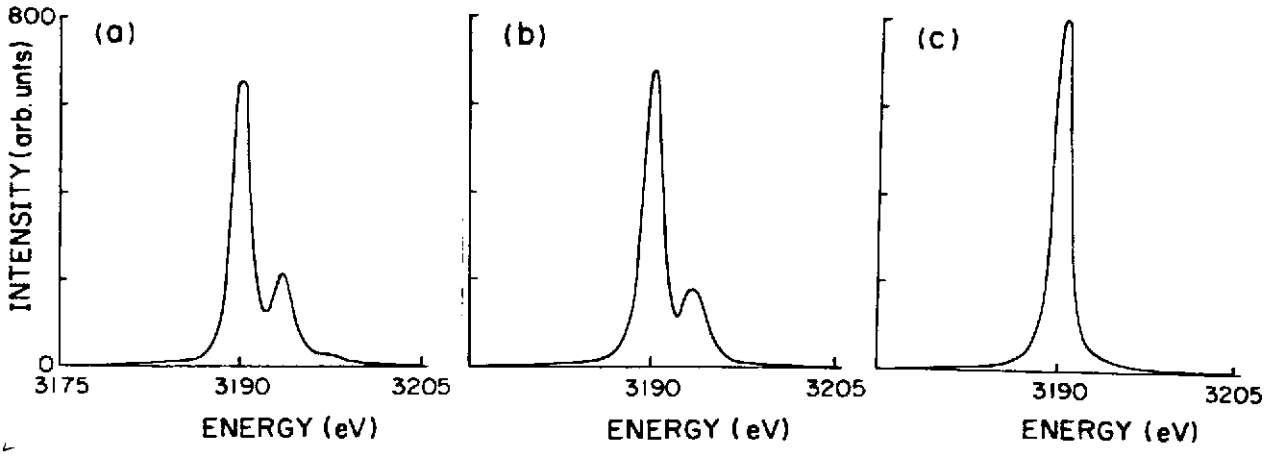

Figure 4
Ar Kβ emission spectra obtained with incident photon energy at (a) 3281.4 eV, (b) 3245.9 eV, (c) 3213.1 eV (from ref. 10)

TARGET

The preparation of the atomic or molecular target often is a difficult task. This especially holds for systems not stable under normal conditions. The possibility to form clusters in supersonic beams has opened up a fascinating field for photoionization studies.

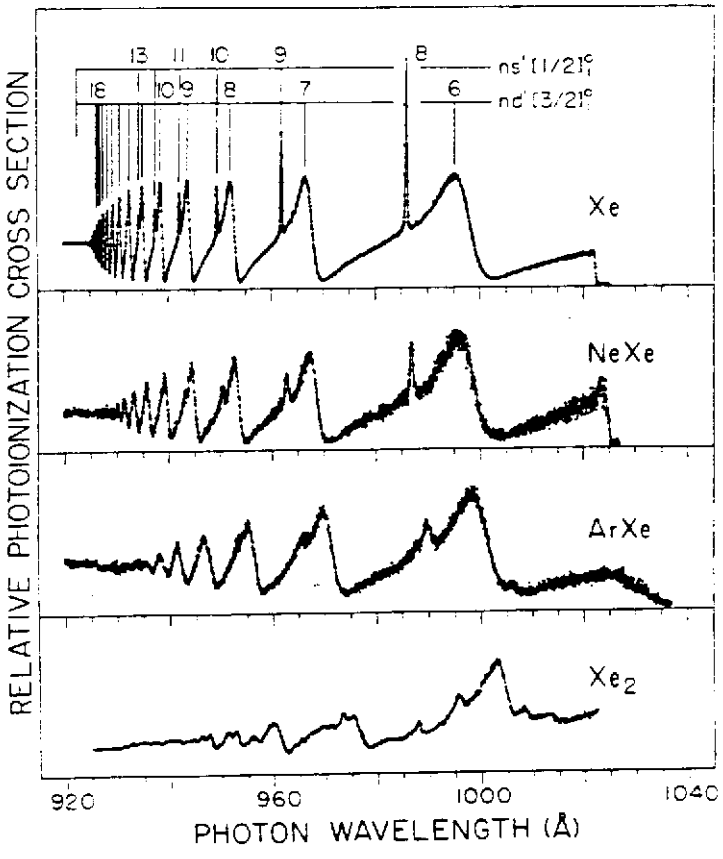

Figure 5
Relative photoionization spectra of Xe, NeXe, ArXe and Xe_2 (from Ref. 1...

The investigation of the Rydberg states of homonuclear and heteronuclear rare gas dimers (14, 15) is a good example for this. The Rydberg states converging towards the ground state of the ion and possibly higher excited states of the ion are prototypes of Rydberg states of weakly bound molecules. Fig. 5 shows the relative photoionization cross sections for Xe, NeXe, ArXe and Xe_2 in the energy region between the $^2P_{3/2}$ and $^2P_{1/2}$ fine-structure thresholds. The spectra have been obtained by photoionization mass spectrometry (14, 15, 16). Since the Franck-Condon overlap between the ground state of the neutral molecule and the ground state of the ion is poor close to the ionization threshold the spectra are dominated by autoionization. Fig. 5 shows a striking example of the progression from a spectrum that shows a strong resemblance to the atomic spectrum (NeXe) to a spectrum that only shows modest resemblance to the atomic spectrum (Xe_2). A supersonic nozzle beam has also been successfully used in recent photoelectron studies of simple hydrogen-bonded dimers (17, 18). The preparation of free (3d, 4d, 5d) transition metal atoms and free rare earths atoms requires very high temperatures which renders most experiments very difficult. On the other hand these

open shell atoms are of great interest from both a theoretical and a practical point of view. During the last years several groups have succeeded to push the upper temperature limit for atomic targets used in VUV and X-ray spectroscopy towards higher and higher values (see e.g. 5 and references therin 19, 20, 21). Fig. 6 shows the intensity of the NiII $3d^9 4s^2\,{}^2H\,{}^2D$ and NiII $3d^8 4s^2\,{}^2P\,{}^2G$ photoemission lines as a function of photon energy (22). Both lines are strongly enhanced in the region of the $3p \rightarrow 3d$ excitations due to the coupling of the $3p^6 3d^8 4s^2\,{}^3F \rightarrow 3p^5 3d^9 4s^2\,{}^3F$ (64,3 eV) ${}^3D$, ${}^3P$ (68,5 eV) transitions with the $3p^6 3d^8 4s^2\,{}^3F \rightarrow 3p^6 3d^7 4s^2\,{}^2H\,{}^2D\,\varepsilon f$ transitions and the coupling of the $3p^6 3d^9 4s\,{}^3D \rightarrow 3p^5 3d^{10} 4s\,{}^3P$ transitions with the $3p^6 3d^9 4s\,{}^3D \rightarrow 3p^6 3d^8 4s\,{}^2P\,{}^2G\,\varepsilon f$ transitions, respectively.

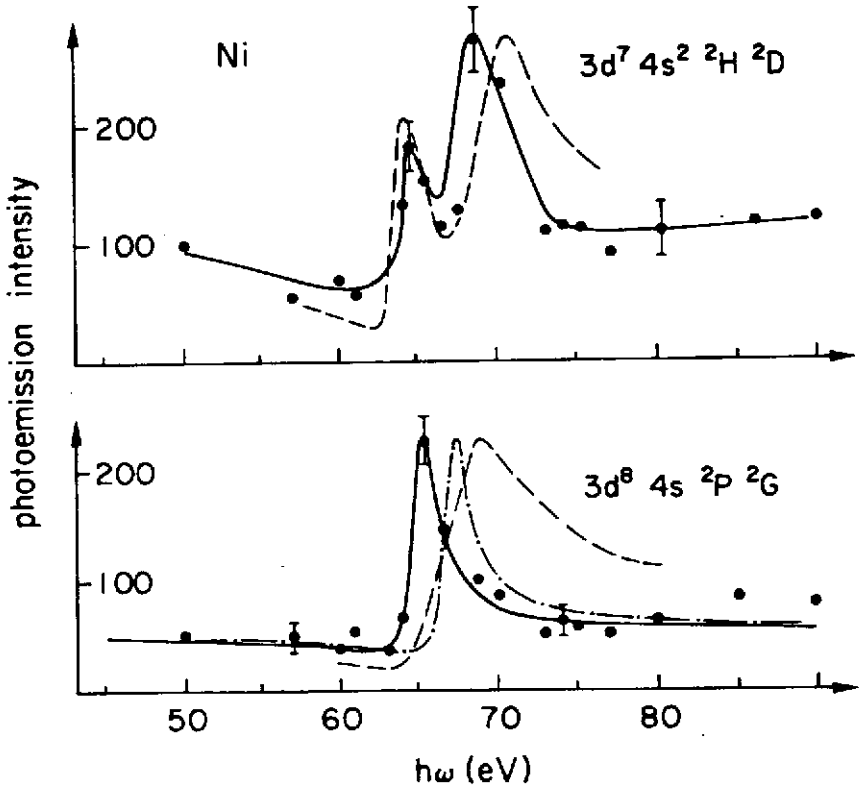

Figure 6
Experimental (full dots) and theoretical (dot-dashed line Ref. 24 dashed Ref. 25) photoemission intensity

The interference between the different excitation channels manifests itself in the Fano type line shape (23) displayed in Fig. 6. The cross section of the NiII $3d^8 4s^2\,{}^2P\,{}^2G$ photoemission line (lower part of Fig. 6) is in fair agreement with the $Ni^+\,\sigma_{3d}$ cross section for the $3p^6 3d^8 \varepsilon f, \varepsilon p$, ${}^2P$ final state calculated by using the reaction matrix theory (24). Fitting the experimental spectrum by the Fano profile

$$\sigma = \sigma_a \frac{(q+\varepsilon)^2}{1+\varepsilon^2} + \sigma_b \quad , \qquad \varepsilon = \frac{E - E_r}{\Gamma}$$

for the interaction of one discrete state with several continua we obtain a value of 3.3 ± 0.3 for the profile index q, a value of 0.9 ± 0.2 eV for the half-width Γ of the line and a value of 65.0 ± 0.2 eV for the position E_r of the autoionizing level. These values for q and Γ compare favourably with the calculated values q = 2.945 and Γ = 0.86 eV. The theoretical position of the resonance E_r = 66.99 eV lies 2 ± 0.2 eV above the experimental value. Part of this difference may be due to the shift of the resonance energy when going from Ni^+ to neutral Ni. The results of model calculations (25) fairly well describe the characteristic features of the spectra, though they overestimate Γ and underestimate q. Similar resonances have been observed in the photoemission spectra of atomic Eu for photon energies close to the 4d and 3d thresholds (26). This experiment demonstrated that, inspite of the smaller cross sections, resonant photoemission spectroscopy on free metal atoms is possible now up to photon energies of ~1000 eV.

The interaction of photons with atoms or molecules in a well defined excited state is of fundamental interest. Lasers are very apt to create a steady population of atoms and molecules in an excited state. The first results obtained by the combined use of lasers and synchrotron radiation for excited state spectroscopy are very promising (see Ref. 5 and references therein, 27). These new type of experi-

ments open new frontiers for exploring the geometrical and dynamical properties of atoms and molecules from states hitherto inaccessible.

MASS SPECTROSCOPY

In light elements like C, N and O a core hole created by photoabsorption decays preferentially via an Auger KLL transition. If these atoms are bound in molecules this process results in highly charged molecules which are unstable and fall apart in a Coulomb explosion. Recently the fragmentation of CO and $(CH_3)_2$ CO, caused by C1s excitation has been investigated (28). The fragmentation pattern was shown to change whether the C1s electron gets ionized or excited into a Rydberg-orbital or into an antibonding π^* molecular orbital. Furthermore the fragmentation depends on the site of the carbon atom that has been excited. This suggests the use of soft X-rays to stimulate chemical reactions or to selectively break organic molecules. High resolution photoionization mass spectroscopy is well suited for the investigation of electron-correlation phenomena. This is corroborated by the recent results on atomic (Ba (29), Cl and F (30). The complex interactions among the various BaI, BaII and BaIII states and their associated continua in the region of the 5p excitation have also prompted new photoemission (31) and photoabsorption (32) measurements.

VIBRATIONALLY RESOLVED PHOTOELECTRON SPECTROSCOPY

Vibrationally resolved photoelectron spectroscopy has contributed considerably to the understanding of molecular photoionization processes (4, 5, 33, 34) Non Franck-Condon effects caused by shape resonances or autoionization clearly manifest themselves in the vibronic partial cross sections, (35, 36, 37). The ionization of a $3\sigma_g$ valence electron in O_2 shows both effects, though the identification of the shape resonance in the σ_u^2 channel is complicated by the overlapping autoionization structure. Because of the open $1\pi_g$ shell the ejection of a $3\sigma_g$ electron leads to two ionic states $b^4\Sigma_g^-$ and $B^2\Sigma_g^-$. A broad maximum shows up at 21.5 eV in the total and vibrationally resolved partial photoionization cross sections for the $b^4\Sigma_g^-$ and the $B^2\Sigma_g^-$ state of O_2^+ (38). Energy position, width and dependence on vibrational quantum number are consistent with the interpretation as a shape resonance. The total and vibrationally resolved partial photoionization cross sections for the $b^4\Sigma_g^-$ state of O_2^+ in the range 18.17 - 21 eV photon energy range display large structures caused by Rydberg series converging towards the B state which decay primarily into the b ionization continuum (Fig. 7).

Strong differences can be recognized for different final vibrational ion states. Similar geometries of both autoionizing states and final ionic states, which leads to a $\Delta v = 0$ propensity rule, explain the vibrational selectivity. Strong valence-Rydberg orbital mixing is responsible for the exceptionally wide $4p\sigma_u$ peak at 19 eV. The MQDT calculations fairly well reproduce the characteristic features of the experimental spectra.

ROTATIONALLY RESOLVED PHOTOELECTRON SPECTROSCOPY

Even with state-of-the-art electron energy analysis, with the application of molecular beams to reduce the Doppler effect and with resonance line sources optimized for narrow linewidth the resolution of single rotational transitions is only possible for very few molecules. New results have been reported on H_2 (39, 40), HD and D_2 (39). As an example results of fit calculations for the rotational structure of the H_2^+ (v' = 0) vibrational peak in the 58.4 nm, 73.6 nm and 74.4 nm photoelectron spectrum of H_2 are given in Fig. 8 (40). The thick lines represent the sum of the individual rotational components (thin lines). The bars in the lower part of the figure show the difference between the fit and the data points on the same intensity scale. Each vibrational peak is composed mainly of four rotational transitions $J'' \rightarrow J'$ (0→0, 0→2, 1→1, 1→3) with small additions from the 2→2 and 3→3 transitions. The rotational cross sections ratios σ_s/σ_Q are in most cases by about a factor of 2 smaller than predicted by theoretical calculations. On the other hand the precise ionic and vibrational constants determined by this high resolution measurements (39) are consistent with the available theoretical rotation-vibration energy levels.

Figure 7
Total and vibrationally resolved partial photoionization cross sections (dots; experiments; solid line MQDT) for the $b^4\Sigma_g^-$ state of O_2^+ (from Ref. 38)

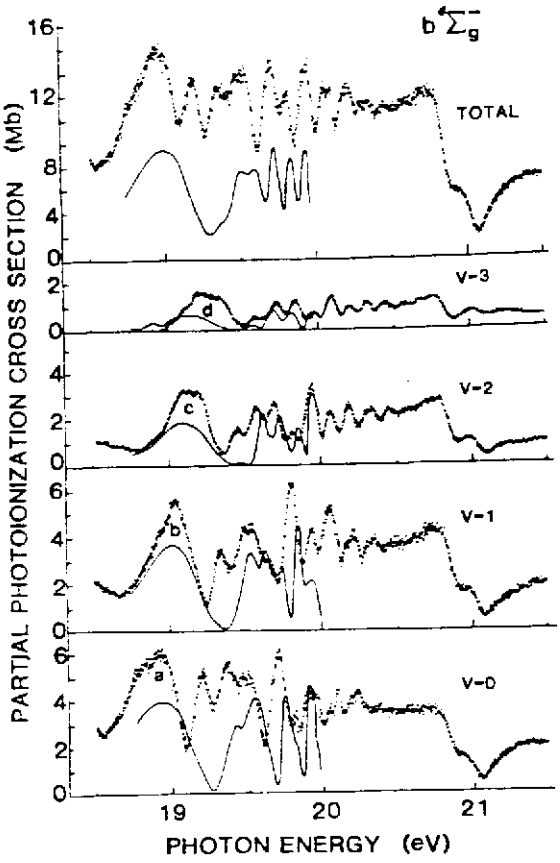

Figure 8
Rotational structure of the H_2^+ (v' = 0) vibrational peak obtained by fit calculations (from ref. 40)

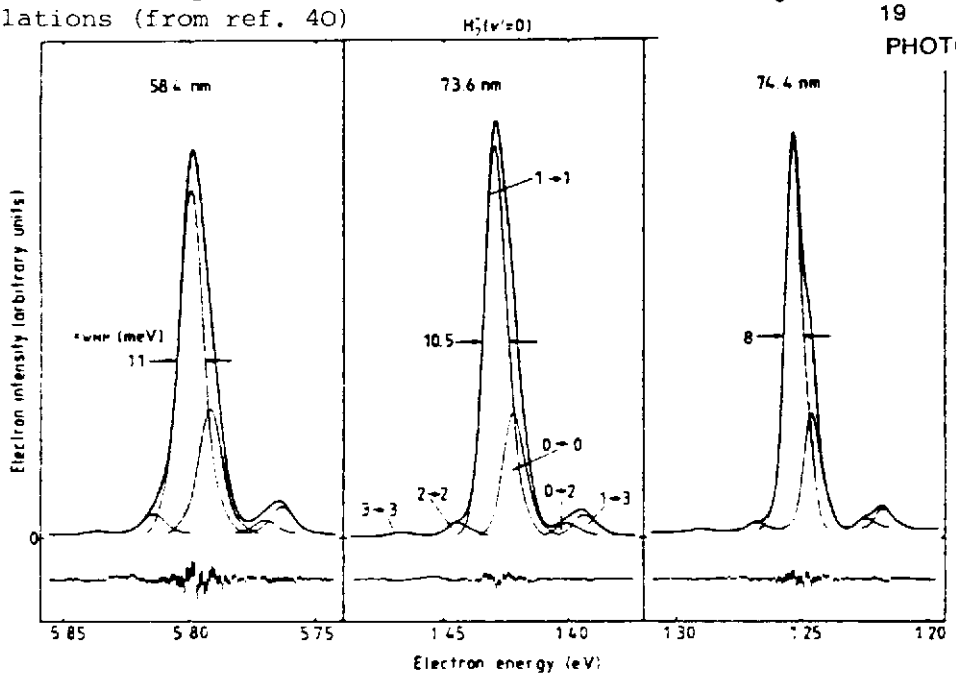

ANGULAR AND ENERGY RESOLVED PHOTOELECTRON SPECTROSCOPY

For randomly oriented atoms or molecules the photoejection by electric dipole interaction with partly polarized (P degree of polarization) radiation is described by a differential cross section of the form

$$\frac{d\sigma}{d\Omega} = \frac{\sigma}{4\pi}\left\{1+\frac{3}{4}\beta\left[(1+P)\cos^2\Theta_x + (1-P)\cos^2\Theta_y - \frac{2}{3}\right]\right\}$$

The photon beam propagates along the Z-axis and the angles Θ_x and Θ_y refer to the direction of the photoelectron with respect to the x and y axes. Since the asymmetry parameter depends on the size of the dipole matrix element and on the phase of the final state wave function, the experimental determination of β forms a stringent test for theoretical models. This explains the great effort devoted to this type of measurements (1, 2, 4, 5, 6 Kr and Xe 41; Cd 42, Hg 43; Xe 44, 45, 46, Ga 47, O_2 35; CO_2 36; C_2H_2 48, 49; ethylene 50; CO 51; H_2O 52, N_2O 53; SF_6 54; SiF_6, $Si(CH_3)_4$ 55). The simple two-electron structure of H_2 has made it a prototype system. The marked discrepancies between the various experimental and calculated β values signal the difficulties encountered both in theory and in experiment (40, 56, 57). It is clear from the existing results, that the outgoing wave is not of pure p character but contains a significant admixture of f character.

In atomic physics the studies of the outer s shell photoemission of rare gases has turned out to be a crucial test for theoretical models. The Cooper-Zare model gives a value of 2 for the Xe5s angular asymmetry parameter, independent of photon energy. Relativisatic and correlation effects cause a strong deviation from the value of 2 close to the Cooper minimum. The present state is summarized in Fig. 9. The experimental data (open circles Ref. 46, full circles Ref. 45, squares Ref. 58, triangle Ref. 59) show a marked minimum of β at the Cooper minimum. This minimum is also present in the theoretical β-curves, but the K-matrix calculations (60) underestimate the depth of the minimum whereas the RRPA calculations (61) overestimate it. The latter result is of special interest since the experimental partial 5s cross section is in reasonable agreement with the predictions of the RRPA calcuations.

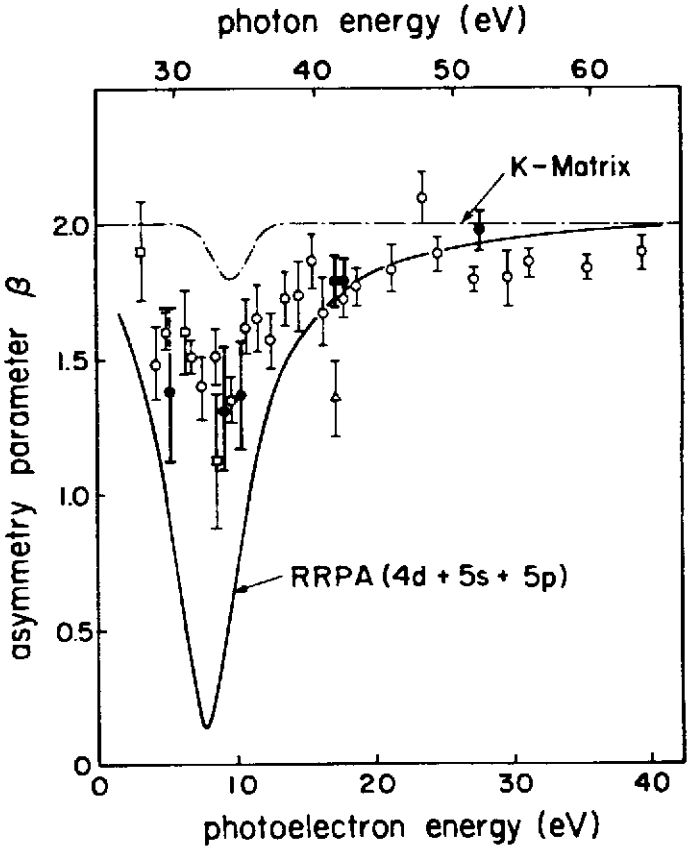

Figure 9
Photoelectron angular asymmetry parameter β for the 5s subshell of Xe.

For a complete characterization of an atomic photoionization process in addition to the total and partial cross sections and the asymmetry parameter β further parameters are necessary. Angle-, energy- and spin-resolved photoemission experiments can yield the spin parameters ζ, A and α, (62, 63, 5 and references therein). For the Xe 5p excitation all these parameters have been determined recently (64).

ALIGNMENT IN ELECTRON SPECTROSCOPY

Photoemission can result in an unequal population of the magnetic sublevels JM of the ion (65). The alignment of the ion is reflected in the anisotropic angular distribution of the electrons emitted in the subsequent Auger decay. The Auger electron angular distribution takes the form

$$I(\Theta) \sim 1 + P_2(\cos\Theta),$$

where Θ is measured with respect to the photon polarization vector. The asymmetry parameter is proportional to the alignment tensor of the initial state of the Auger transition;

$$\beta(\varepsilon) = A_{20}(\varepsilon),$$

ε represents the kinetic energy of the photoelectron. In the two-step model the energy dependence of the Auger electron asymmetry is determined only by the alignment tensor $A_{20}(\varepsilon)$, which is a property of the inner-shell hole state. α describes the Auger decay and therefore depends on the final state reached by the Auger decay. According to the above equation, the asymmetry parameters of all Auger transitions starting from the same inner-shell vacancy state should display the same photon-energy dependence. Recently the angular distribution of the electrons created by the

$$Xe^+(4d^9 5s^2 5p^6\, ^2D_{5/2}) \rightarrow Xe^{++}(4d^{10} 5p^6\, ^1S_0) + e^-(\varepsilon d)$$

$$Xe^+(4d^9 5s^2 5p^6\, ^2D_{5/2}) \rightarrow Xe^{++}(4d^{10} 5s5p^5\, ^1P_1) + e^-(\varepsilon p, \varepsilon f)$$

Auger decays have been determined experimentally (66, 67). The initial 4d-hole states have been prepared by photoionization:

$$Xe(4d^{10}5s^{2}5p^{6}\,{}^{1}S_{0}) + \hbar\omega \rightarrow Xe^{+}(4d^{9}5s^{2}5p^{6}\,{}^{2}D_{5/2}) + e^{-}(\varepsilon p, \varepsilon f)$$

The Auger electron asymmetry parameters for the Xe $N_5O_1O_2\,{}^{1}S_0$ (open circles) and $N_5O_1O_{2,3}\,{}^{1}P_1$ (closed circles) are given in Fig. 10.

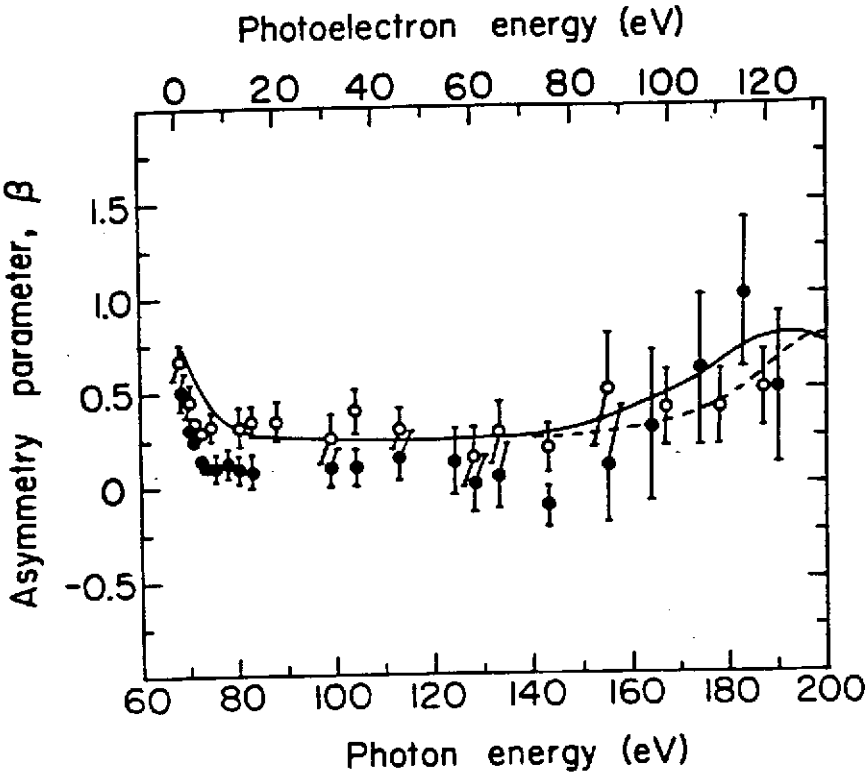

Figure 10
Auger electron asymmetry parameters for the transitions Xe $N_5O_1O_1\,{}^{1}S_0$ and Xe $N_5O_1O_2\,{}^{3}P_1$ (from Ref. 67)

For the Xe^{++} $(4d^{10}5p^{6}\,{}^{1}S_0)$ final state there is a single continuum wave. In this simple case α is given by a product of angular momentum coupling coefficients (68). β can expressed by

$$\beta(N_5O_1O_1\,{}^{1}S_0) = 4\sqrt{\frac{2}{7}}\,A_{20}$$

and thus the alignment tensor can be determined directly from the experimental asymmetry parameter. The value of A_{20} is determined by the photoionization matrix elements. In the nonrelativistic limit transitions of the 4d electron to εp and εf continuum waves contribute to photoionization. Theoretical analysis (65, 69) shows that A_{20} is determined by the partical branching ratio

$$\gamma(\varepsilon) = \frac{(4d \rightarrow \varepsilon p)}{(4d \rightarrow \varepsilon f)},$$

In an independent particle model the Xe4d partial branching ratio is given by

$$\gamma(\varepsilon) = \frac{2R^{2}4d\varepsilon p}{3R^{2}4d\varepsilon f},$$

where R stands for the radial dipole matrix elements. Inserting calculated values (70) of the partial branching ratio into the formula (69)

$$A_{20} = \frac{2}{7}\,\frac{1+\frac{7}{2}\gamma}{5(1+\gamma)}$$

the alignment tensor has been calculated (61) for $Xe^{+}(4d^{9}5s^{2}5p^{6}\,{}^{2}D_{5/2})$. The $\beta(N_5O_1O_1\,{}^{1}S_0)$ values obtained from these A_{20} values are included in Fig. 10. The solid (dashed) line is based on HF-dipole matrix elements obtained in the velocity (length) approximation. The experimental data follow the calculated Auger electron asymmetry parameter. The Auger asymmetries are large close to the 4d ionization threshold were the $4d \rightarrow \varepsilon f$ transitions are supprensed by the centifugul barrier in the f-wave effective potential. Large Auger asymmetries are also produced near the Cooper minimum in the f-wave channel. Higher resolution measurements for photonen energies 68 eV $\leq \hbar\omega \lesssim$ 82 eV (61) show that the $N_{45}O_1O_1\,{}^{1}S_0$, $N_{45}O_1O_{2,3}\,{}^{1}P_1$ and $N_{45}O_{23}O_{23}(^{2}P)5d\,{}^{1}P_1$ Auger lines have about the same β values, i.e., their Auger decay parameters α do not differ greatly.

Before turning toward fluorescence spectroscopy we want to refer to recent results on molecular photoemission (71, 72).

ALIGNMENT IN FLUORESCENCE SPECTROSCOPY

The polarization of fluorescence from excited state atomic or molecular photoions provides a direct measure of their alignment, and thus the relative dipole strength of degenerate excitation channels (73, 74). Hence fluorescence polarization can be used to characterize the symmetry signatures and dynamical properties of autoionizing resonances. The process

$$CO_2(X\,^1\Sigma_g^+) + \hbar\omega \xrightarrow[-1\pi_u]{-3\sigma_u} \begin{cases} CO_2^*(R) \\ CO_2^+(A\,^2\Pi_u) + e^-(\varepsilon\sigma_g, \varepsilon\pi_g, \varepsilon\delta_g) \\ CO_2^+(X\,^2\Pi_g) + \hbar\omega' \end{cases}$$

recently studied (75) serves as a good example R denotes a Rydberg state; $-3\sigma_u$ an $-1\pi_u$ indicate which electron is excited. The experiment was carried out by scanning the excitation photon energy $\hbar\omega$ and measuring the polarization of the undispersed CO_2^+ $A^2\Pi_u \rightarrow X^2\Pi_g$ fluorescence. The results are shown in Fig. 11.

The excitation spectrum, taken with the polarizer removed, shows extensive autoionization structure. The fluorescence polarization spectrum shows analogous structure, supersimposed on a non-resonant background. The degree of polarization P is given by

$$P = \frac{3\cos^2\alpha - 1}{\cos^2\alpha + 3}$$

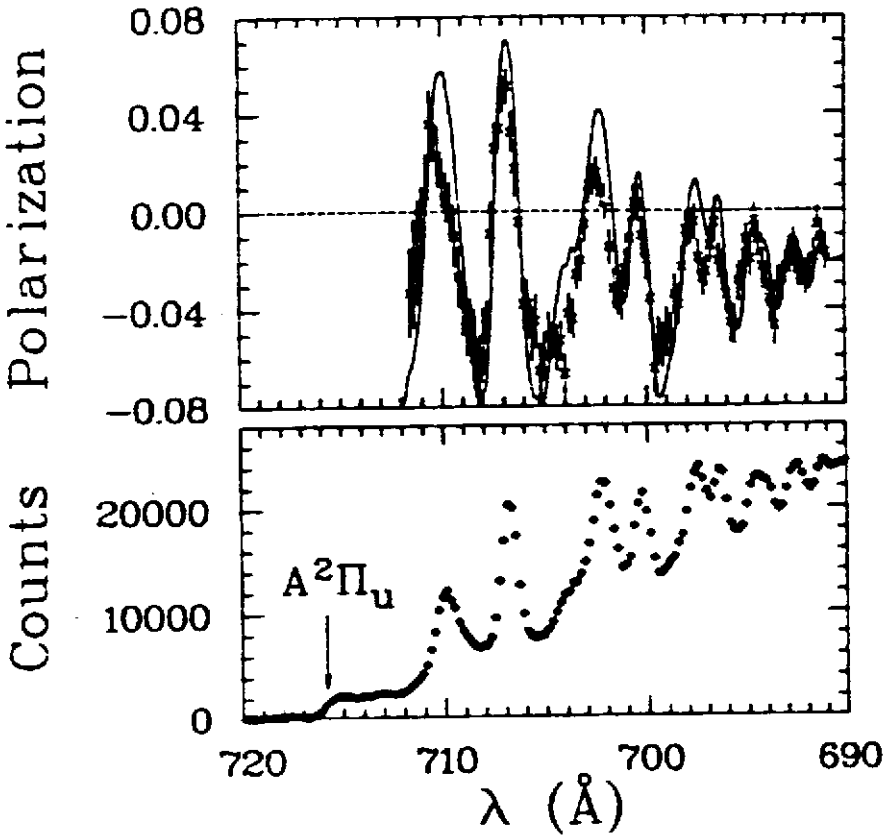

Figure 11
Excitation spectrum (bottom) and polarization profile (top) for the A→X fluorescence from CO_2^+, (from Ref. 75)

where α is the angle between the absorption and fluorescence transition dipoles (76). The polarization $P = -0.07 \pm 0.1$ of the non resonant background is consistent with the assignment of the nonresonant excitation to $1\pi_u \rightarrow \varepsilon\delta g$ photoionization. Good agreement with the polarization data has been achieved by assuming the resonant features emanate from a $^2\Sigma_u^+$ Rydberg state. In this case the transition dipoles are parallel to the intermolecular axis for both absorption and fluorescence, leading to P = 0.143 for the resonant contributions. The solid line in the topframe of Fig. 11 represents the P predicted from the excitation spectrum, based on a simple weighted average of resonant and nonresonant contributions at each wavelength.

Recent fluorescent excitation spectra have been reported for N_2O (77) and N^2 (78). For N_2 there exist also preliminary results for fluorescence excitation studies

of photoionization in external electric fields (79).

The wealth of information which can be obtained by coincidence experiments has hardly been tapped (80, 81, 82). With the increase of the intensities of the light sources the number of experiments of this type will grow considerably.

REFERENCES

1) J.A.R. Samson, Atomic Photoionization Handbuch der Physik, Vol. 31, ed. W. Mehlhorn (Springer Verlag, Berlin, 1982) p. 123
2) A.F. Starace, Theory of Atomic Photoionization, Handbuch der Physik, Vol. 31, ed. W. Mehlhorn (Springer Verlag, Berlin, 1982) p. 1
3) E.E. Koch and B.F. Sonntag, in Synchrotron Radiation; Techniques and Applications, ed. C. Kunz (Springer Verlag, Heidelberg, 1979) p. 269
4) J.L. Dehmer, D. Dill and A.C. Parr in Photophysics and Photochemistry in the Vacuum Ultraviolet ed. S. McGlynn, G. Findley and R. Huebner (D. Reidel Publ. Comp., Dordrecht, Holland 1983)
5) B.F. Sonntag and F. Wuilleumier, Nucl. Instr. Meth. 208, 735 (1983)
6) Proceeding of the Intern. Conf. on X-Ray and VUV Synchrotron Radiation Instrumentation, Nucl. Instr. Meth. 208 (1983)
7) E.E. Koch and D.E. Eastman in Handbook on Synchrotron Radiation, Vol. 1, ed. E.E. Koch (North Holland 1983)
8) R. Hilbig and R. Wallenstein, IEEE Journal of Quantum Electronics, 19, 194 (1983)
9) G. Brown, K. Halbach, J. Harris and H. Winick, Nucl. Instr. Meth. 208 (1983)
10) R.D. Deslattes, R.E. Lavilla, P.L. Cowan and A. Henins, Phys. Rev. A 27, 923 (1983)
11) J.B. Hasting, B.M. Kincaid and P. Eisenberger, Nucl. Instr. Meth. 152, 167 (1978)
12) J.M. Esteva, B. Gauthé, P. Dhez and R.C. Karnatak, J. Phys. B 16, L 263 (1983)
13) M.H. Tuilier, D. Laporte and J.M. Esteva, Phys. Rev. A 26 372 (1982)
14) P.M. Dehmer and S.T. Pratt in Photophysics and Photochemistry in the Vacuum Ultraviolet, ed. S. McGlynn, G. Findley and R. Huebner, (D. Reidel Publ. Comp., Dordrecht, Holland 1983)
15) P.M. Dehmer, Comments on Atomic and Molecular Physics, to be published
16) P.M. Dehmer and S.T. Pratt, J. Chem. Phys. 77 4804 (1982)
17) Sh. Tomoda, Y. Achiba, K. Nomoto, K. Sato and K. Kimura, Chem. Phys. 74, 113 (1983)
18) Sh. Tomoda and K. Kimura, Chem. Phys. 74, 121 (1983)
19) J.M. Dyke, B.W.J. Gravenor, R.A. Lewis and A. Morris, J. Phys. B 15, 4523 (1982)
20) M. Pantelouris and J.P. Connerade, J. Phys. B 16, L 23 (1983)
21) G. Materlik, B. Sonntag and M. Tausch, to be published
22) E. Schmidt, H. Schröder, B. Sonntag, H. Voss and H.E. Wetzel, J. Phys. B, to be published
23) U. Fano, Phys. Rev. 124, 1866 (1961)
24) F. Combet-Farnoux and M. Ben Amar, Phys. Rev. A 21, 1975 (1980)
25) L.C. Davis and L.A. Feldkamp, pricate communication
26) U. Becker and D.A. Shirley, private communication
27) F. Wuilleumier, J. Physique 43, C2 - 347 (1982)
28) W. Eberhardt, T.K. Shahm, R. Carr, S. Krummacher, M. Strongin, S.L. Wong and D. Wesner, Phys. Rev. Lett. 50, 1038 (1983)
29) B. Lewandowski, J. Ganz, H. Hotop and M.W. Ruf, J. Phys. B 14, L 803 (1981) and M.W. Ruf, private communication
30) B. Ruscic and J. Berkowitz, Phys. Rev. Lett. 50, 675 (1983)
31) P.H. Kobrin, R.A. Rosenberg, U. Becker, S. Southworth, C.M. Truesdale, D.W. Lindle, G. Thornton, M.G. White, E.D. Poliakoff and D.A. Shirley, to be published
32) M.A. Baig and J.P. Connerade, to be published
33) P. Morin, I. Nenner, P.M. Guyon, L.F.A. Ferreira and K. Ito, Chem. Phys. Lett. 92, 103 (1982)
34) I. Nenner, Proceedings of the "Photochemistry and Photobiology Conference", Alexandria (1983) and J. of Laser Chemistry, to be published

35) P.M. Dittman, D. Dill and J.L. Dehmer, J. Chem. Phys. 76, 5703 (1982)
36) A.C. Parr, D.L. Ederer, J.L. Dehmer and D.M.P. Holland, 77, 111 (1982)
37) A.C. Parr, D.L. Ederer, J.B. West, D.M.P. Holland and J.L. Dehmer, J. Chem. Phys. 76, 4349 (1982)
38) P. Morin, I. Nenner, M.Y. Adam, M.J. Hubin-Franskin, J. Delwiche, J. Lefebvre-Brion and A. Giusti-Suzor, Chem. Phys. Lett. 92, 609 (1982)
39) J.E. Pollard, D.J. Trevor, J.E. Reutt, Y.T. Lee and D.A. Shirley, J. Chem. Phys. 77 34 (1982) and Chem. Phys. Lett. 88, 344 (1982)
40) M.W. Ruf, T. Bregel and H. Hotop, J. Phys. B 16, 1549 (1983)
41) D.L. Ederer, A.C. Parr, J.B. West, D. Holland and J.L. Dehmer, Phys. Rev. A 25 2006 (1982)
42) P.H. Kobrin, U. Becker, S. Southworth, C.M. Truesdacle, D.W. Lindle and D.A. Shirley, Phys. Rev. A 26, 842 (1982)
43) P.H. Kobrin, P.A. Heimann, H.G. Kerkhoff, D.W. Lindle, C.M. Truesdale, T.A. Ferrett, U. Becker and D.A. Shirley, Phys. Rev. A (to be published)
44) S. Southworth, U. Becker, C.M. Truesdale, P.H. Kobrin, D.W. Lindle, S. Owaki and D.A. Shirley, Phys. Rev. A (to be published)
45) H. Derenbach and V. Schmidt, J. Phys. B 16 L 337 (1983)
46) A. Fahlmann, Th.A. Carlson and M.O. Krause, Phys. Rev. Lett. 50, 1114 (1983)
47) M.O. Krause, F. Cerrina and A.F. Fahlmann, Phys. Rev. Lett. 50, 1118 (1983)
48) D.M.P. Holland, J.B. West, A.C. Parr, D.L. Ederer, R. Stockbauer and J.L. Dehmer, J. Chem. Phys. 78, 124 (1983)
49) P.R. Keller, D. Mehaffy, J.W. Taylor, F.A. Grimm and T.A. Carlson, Journ. Electr. Spectr. and Rel. Phen. 27, 223 (1982)
50) D. Mehaffy, P.R. Keller, J.W. Taylor, T.A. Carlson, M.O. Krause, F.A. Grimm and J.D. Allen, Journ. Electr. Spectr. and Rel. Phen. 26, 213 (1982)
51) C.M. Truesdale, S.H. Southworth, P.H. Kobrin, U. Becker, D.W. Lindle, A.G. Kerkhoff and D.A. Shirley, Phys. Rev. Lett. 50 1265 (1983)
52) C.M. Truesdale, S. Southworth, P.H. Kobrin, D.W. Lindle, G. Thornton and D.A. Shirley, J. Chem. Phys. (to be published)
53) C.M. Truesdale, S. Southworth, P.H. Kobrin, D.W. Lindle, and D.A. Shirley, J. Chem. Phys. (to be published)
54) J.L. Dehmer, A.C. Parr, S. Wallace and D. Dill, Phys. Rev. A 26 3283 (1982)
55) P.R. Keller, J.W. Taylor, F.A. Grimm, P. Senn, T.A. Carlson and M.O. Krause, Chem. Phys. 74 247 (1983)
56) S. Southworth, W.D. Brewer, C.M. Truesdale, P.H. Kobrin, D.W. Lindle and D.A. Shirley, Journ. Electr. Spectr. and Re. Phen. 26, 43 (1982)
57) Y. Itikawa, H. Takagi, H. Nakamura and H. Sato, Phys. Rev. A 27 1319 (1983)
58) M.G. White, S.H. Southworth, P.H. Kobrin, E.D. Poliakoff, R.A. Rosenberg and D.A. Shirley, Phys. Rev. Lett. 43, 1661 (1979)
59) J.L. Dehmer and D. Dill, Phys. Rev. Lett. 37, 1049 (1976)
60) K.N. Huang and A.F. Starace, Phys. Rev. A 19, 2335 (1980)
61) W.R. Johnson and K.T. Cheng, Phys. Rev. Lett. 40, 1167 (1978) and Phys. Rev. A 20, 928 (1979)
62) G. Schönhense, U. Heinzmann, J. Kessler and N.A. Cherepkov, Phys. Rev. Lett. 48, 603 (1982)
63) F. Schäfers, G. Schönhense and U. Heinzmann, Z. Phys. A 304, 41 (1982)
64) U. Heinzmann and G. Schönhense, private communication and Ch. Heckenkamp, F. Schäfers, G. Schönhense and U. Heinzmann, 7. Intern. Conf. on VUV Radiation Physics, Jerusalem, 1983
65) S. Flügge, W. Mehlhorn and V. Schmidt, Phys. Rev. Lett. 29, 7 (1972)
66) S.H. Southworth, P.H. Kobrin, C.M. Truesdale, D.W. Lindle, S. Owaki and D.A. Shirley, Phys. Rev. A 24, 2257 (1981)
67) S. Southworth, U. Becker, C.M. Truesdale, P.H. Kobrin, D.W. Lindle, S. Owaki and D.A. Shirley, Phys. Rev. (to be published)
68) E.G. Berezhko, N.M. Kabachnik and V.S. Rostovsky, J. Phys. B 11, 1749 (1978)
69) E.G. Berezhko, N.M. Kabachnik, J. Phys. B 10, 2467 (1977)
70) D.J. Kennedy and S.T. Manson, Phys. Rev. A 5, 227 (1972)
71) S. Krummacher, V. Schmidt, F. Wuilleumier, I.M. Bizau and D.L. Ederer, L. Phys. B 16 1733 (1983)
72) B. Ruscic, G.L. Goodman and J. Berkowitz, J. Chem. Phys. 78, 5443 (1983)
73) C.H. Greene and R.N. Zare, Ann. Rev. Phys. Chem. 33, 119 (1982)
74) E.D. Poliakoff, J.L. Dehmer, D. Dill, A.C. Parr, K.H. Jackson and R.N. Zare, Phys. Rev. Lett. 46, 907 (1981)

75) E.D. Poliakoff, J.L. Dehmer, A.C. Parr and G.E. Leroi, J. Chem. Phys. 77, 5243 (1982)
76) McClintock, W. Demtröder and R.N. Zare, J. Chem. Phys. 51, 5509 (1969)
77) P.M. Guyon, T. Baer and I. Nenner, J. Chem. Phys. (to be published)
78) A. Tabche-Fouhaile, K. Ito, I. Nenner, H. Fröhlich and P.M. Guyon, J. Chem. Phys. 77, 182 (1982)
79) E.D. Poliakoff, J.L. Dehmer, A.C. Parr, G.F. Leroi, VUV Conference, Jerusalem, 1983
80) H. Klar and H. Kleinpoppen, J. Phys. B 15, 933 (1982)
81) H. Klar, J. Phys. B 13, 2037 (1980)
82) E.D. Poliakoff, P.M. Dehmer, J.L. Dehmer and R. Stockbauer, J. Chem. Phys. 76, 5214 (1982)

---

to be published in: Book ov Invited Papers XIII Intern. Conf. on the Physics of Electronic and Atomic Collisions, Berlin, July 27-August 2, 1983, ed. by J. Eichler, I.V. Hertel and N. Stolterfoht, North-Holland Publishing Company, Amsterdam.